Available online at www.sciencedirect.com
SCIENCE DIRECT®
Catalysis Today 96 (2004) 265–272
CATALYSIS TODAY
www.elsevier.com/locate/cattod

Operando Raman–GC studies of alumina-supported Sb-V-O catalysts and role of the preparation method

M. Olga Guerrero-Pérez, Miguel A. Bañares*

Instituto de Catálisis y Petroleoquímica (CSIC), Marie Curie 2, E-28049-Madrid, Spain

Available online 24 August 2004

Abstract

The interactions between Sb and V are studied by *operando* Raman–GC methodology during propane ammoxidation in order to understand the effect of the preparation method and reaction conditions on the structure and activity/selectivity of alumina-supported Sb-V-O catalysts. Dispersed V(V) species react with antimony species during propane ammoxidation to form $VSbO_4$; partially reversible transformations towards surface vanadium (V) species may account for the catalytic redox cycle. The catalytic performance is determined by the interaction between Sb and V, which is affected by the preparation method and the reaction conditions.

Keywords: *Operando*; Raman; V-Sb-O; Antimonate; Alumina; Preparation method; Tartrate; In situ; Ammoxidation

1. Introduction

The molecular understanding of the events taking place in the catalysts during reaction is critical for the development of structure–activity/selectivity relationships. The use of techniques that analyze surface catalysts while the reaction is taking place must allow a better understanding of the nature of active species. To give an answer to this necessity of assessing a reliable structure–activity relationship at a molecular level, advanced in situ techniques that combine in situ spectroscopy under genuine reaction conditions with simultaneous activity measurement are appearing [1,2]. The term ''*operando*'' (working in Latin) was proposed to express the methodology that *simultaneously* combines in situ characterization and activity measurement in a single experiment using a catalytically appropriate cell [2–6]. The *operando* cell must be designed free of homogeneous reaction contribution and free of diffusional limitations or any profile; thus, it has to be designed as a reactor that is suitable for in situ studies. Because *operando* methodology combines two measurements in a single experiment, it is appropriate to indicate the techniques involved in such experiment. This work combines Raman spectroscopy with on-line gas chromatography (GC); therefore, the study is referred to as *operando* Raman–GC.

The direct conversion of propane into acrylonitrile by ammoxidation is an alternative route to the conventional propylene ammoxidation since propane is cheaper than propylene. In this reaction, the activation of propane is the limiting step. Acrylonitrile is widely used as intermediate for the preparation of synthetic rubbers, synthetic resins and fibbers. Different catalytic systems have been investigated for this reaction [7,8] Mixed Sb-V-O based catalyst have been found to be one of the most promising formulations [9–13], specially, the Sb-V-O-Al system [9,14–18]. In order to develop more active and selective catalysts for this process, much attention has been paid to elucidate the molecular structure and mode of operation of V-Sb-Al-O and V-Sb-O catalysts.

Mixed V-Sb oxides present different crystalline phases. At stoichiometric composition or in excess of Sb; well-defined antimony oxides (Sb_2O_3 and α-Sb_2O_4) are present. β-Sb_2O_4 is only present when calcinations temperatures are higher than 800 °C [19]. Crystalline vanadium pentoxide is usually present when Sb/V is lower than 1. Vanadium and antimony can react to form a rutile-like vanadium-antimonate phases ($VSbO_4$). Excess antimony oxide promotes

* Corresponding author. Tel.: +34 91 5854788; fax: +34 91 5854760.
E-mail address: mbanares@icp.csic.es (M.A. Bañares).

0920-5861/$ – see front matter © 2004 Elsevier B.V. All rights reserved.
doi:10.1016/j.cattod.2004.06.150

the catalytic properties because antimony oxide migrates to the surface of the $VSbO_4$ during propane ammoxidation [12,20–22]; this would promote the isolation of V-centers, which appear to be active and selective for acrylonitrile formation [10,21]. A large excess of vanadium, in the form of V_2O_5, appears to catalyze the undesired oxidation NH_3 to N_2 [23]. The formation of $VSbO_4$ after calcination is incomplete; it appears that this phase is further formed during propane ammoxidation by reaction of vanadium and antimony oxides that have not reacted during calcination [9,11,24–27]. A previous paper monitors the structural transformations of surface vanadia and surface antimony oxide species by *operando* Raman–GC, it was possible to follow how surface V and Sb oxides interact during reaction to form the active $VSbO_4$ phase [3]. This contribution studies the nature of such interaction by the use of different preparation methods and by the *operando* evaluation of the transformations during reoxidation and during ammoxidation cycles. The activity and structural transformations provide some understanding on the structure-activity relationships of Sb-V-O-based catalysts for propane ammoxidation and the effect of the synthesis method.

2. Experimental and methods

2.1. Preparation of samples

Two alumina-supported mixed Sb-V oxide catalysts were prepared with different methods, depending on the Sb precursor. In the first preparation method, named **1**, Sb_2O_3 (Aldrich) was added to an aqueous solution of NH_4VO_3 (Sigma), this solution was kept under stirring at 80 °C for 50 min, then, γ-Al_2O_3 was added. The resulting solution was dried in a rotatory evaporator at 80 °C. The resulting solid was dried at 115 °C for 24 h and then calcined at 400 °C for 4 h. For the second preparation method, named **2**, the same procedure was used but Sb was added as soluble tartrate complex [28]. Both catalysts were prepared so that the total coverage of V + Sb would correspond to 100% its dispersion limit on alumina, determined by Raman spectroscopy to be of nine atoms of Sb + V per nm^2 of alumina support [15,29]. The dispersion limit, understood as the maximum surface loading of VO_x units that remain dispersed, with no crystalline V_2O_5. The Sb/V atomic ratio was 1. The catalysts are typically named as *x*SbyV/Al-*z*, where *x* indicates the number of Sb + V monolayers, *y* indicates the Sb/V atomic ratio and *z* indicates the preparation method (**1** for the Sb_2O_3 suspension and **2** for the soluble Sb tartrate precursor).

2.2. Activity measurements

Activity measurements were performed using a conventional microreactor with on-line gas chromatograph equipped with a flame ionization and thermal conductivity detector. The correctness of the analytical determinations was checked for each test by verification that the carbon balance (based on the propane converted) was within the cumulative mean error of the determinations (±10%). To prevent the participation of homogeneous reactivity the reactor was designed to minimize gas-phase activation of propane. Tests were made using 0.2 g of sample with particle dimensions in the 0.25–0.125 mm range. The axial temperature profile was monitored by a thermocouple sliding inside a tube inserted into the catalytic bed. Test were made using the following feedstock: 25% O_2, 9.8% propane, 8.6% ammonia in helium. The total flow rate was 20 ml/min corresponding to a gas-space velocity (GHSV) of about 3000 h^{-1}. Yields and selectivities in products were determined on the basis of the moles of propane feed and products, considering the number of carbon atoms in each molecule.

2.3. Raman spectroscopy

The Raman spectra were run with a single monochromator Renishaw System 1000 equipped with a cooled CCD detector (−73 °C) and holographic super-Notch filter. The holographic Notch filter removes the elastic scattering. Such Raman configuration is successfully used in many applications [4,30,31]. The samples were excited with the 514 nm Ar line; spectral resolution was ca. 3 cm^{-1}. The in situ Raman spectra were run under dehydrated conditions for the fresh and used catalysts. The used catalysts have run propane ammoxidation at 480 °C during 20 h, operating at steady state [15]. The *operando* Raman–GC study during propane ammoxidation were obtained under reaction conditions in a home-made reaction cell. It was made using quartz tubing connected to an optical quality quartz cuvette (Scheme 1). Essentially, it is a fixed-bed catalytic reactor with walls that are optically appropriate for in situ Raman spectroscopy. To prevent the participation of homogeneous reactions, the reactor was designed to minimize gas-phase activation of propane (no void volume). Tests were made using 0.2 g of sample with particle dimensions in the 0.25–0.125 mm range. Test were made using the following feed: 25% O_2, 9.8% propane, 8.6% ammonia in helium. The total flow rate was 20 ml/min corresponding to a gas-space velocity (GHSV) of ca. 3000 h^{-1}. Thus, the reaction conditions were identical to those used in the fixed-bed reactor and the activity values obtained in the *operando* reactor were identical to those obtained in the fixed-bed reactor, within experimental error. The activity in the *operando* reaction cell was measured with an on-line gas chromatograph equipped with a flame-ionization and thermal-conductivity detector (Varian 3800). The correctness of the analytical determinations was checked for each test by verification that the carbon balance (based on the propane converted) was within the cumulative mean error of the determinations (±10%). The yield and selectivity values were determined on the basis of the moles of propane feed and products, considering the number of carbon atoms in each molecule. The activity values did not significantly deviate from those

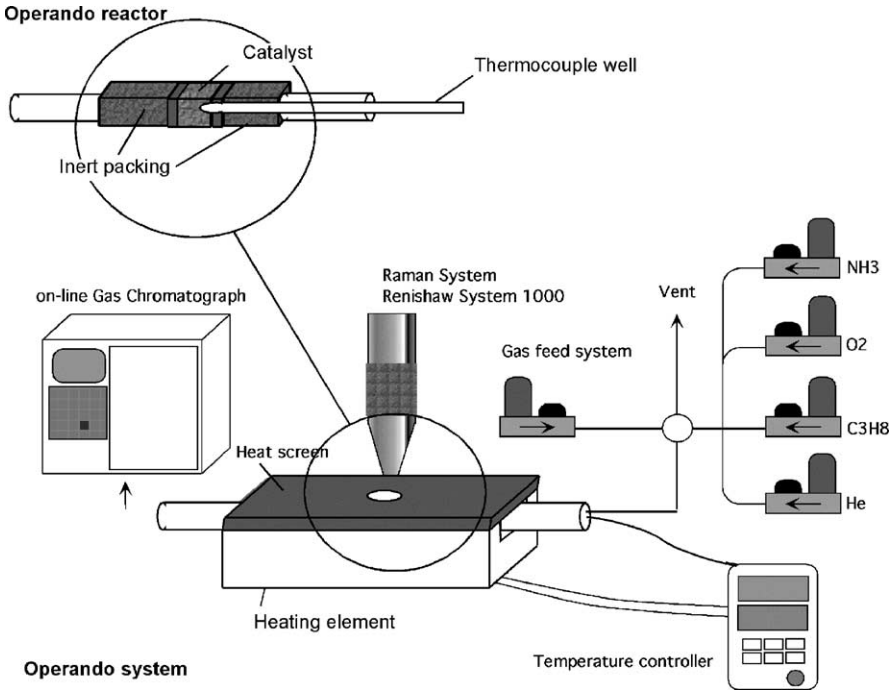

Scheme 1. *Operando* Raman–GC setup.

obtained in the fixed-bed reactor. The laser power on the sample was kept very low (below 6 mW) to prevent local heating at the spot of spectral acquisition, which would have made the spectra not representative of the catalyst bed. As a consequence, the signal-to-noise ratio is low and acquisition time was adjusted to compensate (30 scans of 60 s). Therefore, it was possible to *simultaneously* measure both the structure and the activity/selectivity data *in the same experiment*.

Scheme 2 illustrates the temperature history of the experiments. The first and third cycles correspond to *operando* Raman–GC studies during propane ammoxidation reaction and the second cycle was an in situ re-oxidation (TPO-Raman) experiment. During the Raman–GC studies, each temperature was held long enough (ca. 100 min) to allow, at least, two GC analyses of catalytic activity. Then, it was cooled to 200 °C and the reaction feed is replaced by oxygen–helium feed to run a TPO-Raman study, where the catalyst is heated stepwise from 200 to 520 °C. Spectra are taken at constant temperature. After the reoxidation, the catalyst is cooled down to 200 °C and the second ammoxidation Raman–GC study is carried out.

3. Results

Fig. 1 shows the catalytic results obtained during propane ammoxidation for $1Sb_1V/Al$-1 and $1Sb_1V/Al$-2 catalysts. The catalyst prepared with the tartrate method produces higher amounts of acrylonitrile and lower amounts of pro-

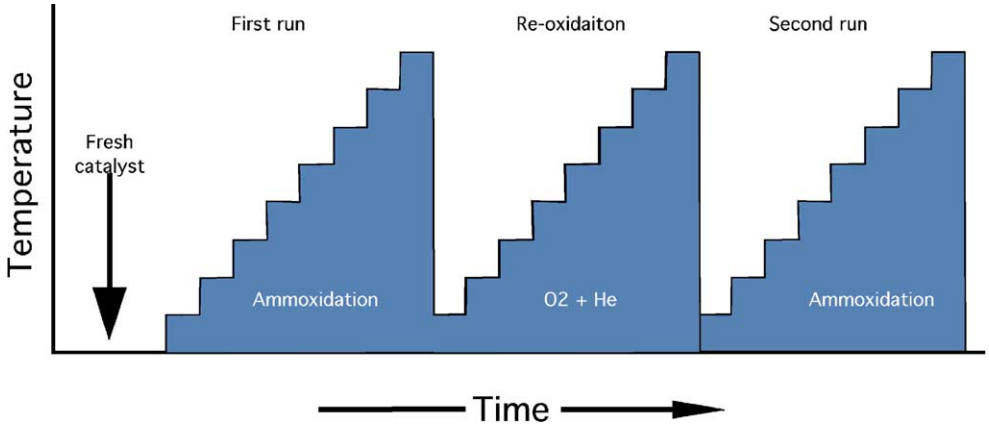

Scheme 2. Temperature profiles during the first successive treatments on catalyst 1Sb1V/Al-1.

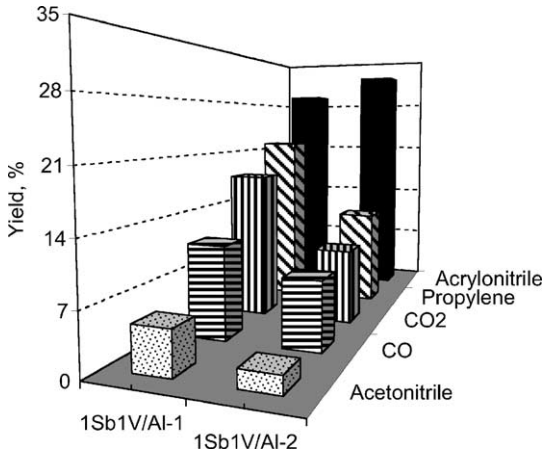

Fig. 1. Yields to principal reaction products for alumina-supported catalysts during propane ammoxidation. Reaction conditions: total flow 20 ml/min; feed composition (% volume): $C_3H_8/O_2/NH_3/He$ (9.8/25/8.6/56.6), 200 mg of catalysts, temperature reaction 480 °C.

pylene, CO_x, and acetonitrile, which makes this catalyst more selective and efficient (acrylonitrile yield 32% versus 29%). The total conversion of propane is also higher for 1Sb1V/Al-2 (tartaric), 85% versus 63%. The BET areas of $1Sb_1V/Al$-1 and of $1Sb_1V/Al$-2 are 117 and 139 m^2/g, respectively. The variation in BET area is not very high. Conversion increases 35% while BET area increases 18%, which would indicate that the better performance is not due to an increase of area. This normalization per area may not be appropriate since the activity depends on surface vanadium oxide species [2,9], which are more difficult to quantify. The preparation method and the reaction conditions may determine the exposure of vanadium sites. Fig. 2 shows the Raman spectra of fresh and used dehydrated catalysts. Fresh $1Sb_1V/Al$-1 catalyst presents a broad Raman band near 900 cm^{-1}, typical of the stretching V-O-V mode surface polymeric vanadium oxide species [4]. Several techniques evidence that antimony is present in the fresh sample (element analysis, XPS) but it does not show Raman bands.

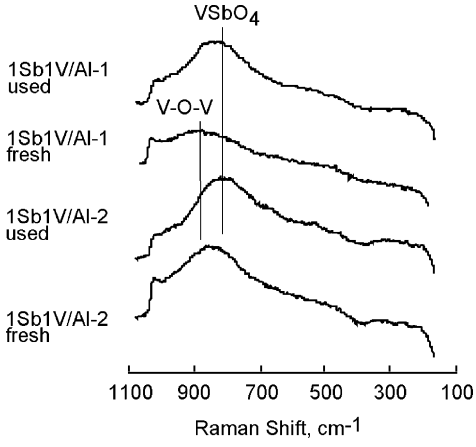

Fig. 2. Raman spectra of dehydrated fresh and used 1Sb1V/Al-1 and 1Sb1V/Al-2 catalysts.

Therefore, it must be dispersed, since surface dispersed antimony oxide species on alumina possess very weak Raman bands [32]; while the corresponding crystalline phases gives rise to strong Raman bands [15]. Thus, the Sb and V oxides appear highly dispersed on the surface of the alumina support for the fresh dehydrated $1Sb_1V/Al$-1 catalyst; after propane ammoxidation, the dehydrated catalyst presents a broad Raman band near 840 cm^{-1}, typical of $VSbO_4$ phase. The Raman spectrum of the fresh $1Sb_1V/Al$-2 shows a band near 1024 cm^{-1}, sensitive to hydration, typical of VO_x surface species. $VSbO_4$ presents two Raman bands, 800 and 840 cm^{-1}; the Raman band near 800 cm^{-1} is more intense than that near 840 cm^{-1} in bulk $VSbO_4$. The formation of $VSbO_4$ on alumina-supported Sb-V-O catalysts after ammoxidation reaction has been observed previously by several techniques [9]. The Raman band near 840 cm^{-1} becomes more intense in supported $VSbO_4$ [33]. Thus, the Raman band near 840 cm^{-1} reflects some distortion in the $VSbO_4$ phase; therefore, it is more defective [33]. The shift of the broad Raman band from 840 to 800 cm^{-1} in the used catalyst must be indicative of a better definition of the Sb-V-O phases. The used catalysts do not form AlSbO4 phase [9], which forms at temperatures significantly higher, 800–900 °C [9]. The $VSbO_4$ phase is present in the fresh catalyst prepared with tartrate complex (method **2**) and in the used catalysts prepared with method **1**. Therefore, *operando* Raman–GC studies were performed in order to understand the mechanism of $VSbO_4$ formation during reaction in the catalyst prepared with the method **1**.

Fig. 3 shows the Raman spectra and simultaneous ammoxidation activity results (i.e., the *operando* study) of $1Sb_1V/Al$-1. Under propane ammoxidation reaction conditions at 200 °C, no important changes of the Raman band of surface vanadium oxide species appear evident. However, as propane conversion becomes measurable, the Raman spectrum shows the broad feature near 800–840 cm^{-1} of the $VSbO_4$ (rutile) phase (15); such band becomes sharper with reaction temperature. At 460 °C, a feature near 190 cm^{-1} evidences the presence of segregated α-Sb_2O_4, which possesses sharp Raman bands at 190, 261, 399, and 459 cm^{-1}, the Raman band at 190 cm^{-1} is the most intense [15]. The weak intensity and the broadness of the Raman band at 190 cm^{-1} suggest that the α-Sb_2O_4 phase must be very incipient and, thus, ill-defined (defective). At 480 °C, the catalyst becomes more selective to acrylonitrile, which corresponds to a transformation of surface vanadia species into incipient $VSbO_4$ and α-Sb_2O_4. This $VSbO_4$ phase generates no X-ray diffraction pattern (thus, its aggregates should not be larger than 4 nm). At lower reaction temperatures, CO_2 and propylene were the main products. As reaction temperature increases, two Raman features near 1060 and 620 cm^{-1} assigned to the V–OC and VO–C stretching vibrations of alkoxy species adsorbed on surface vanadia species, respectively, become apparent [4,34]. Those surface vanadium oxide species appear to be related to propane activation for ammoxidation reaction [2].

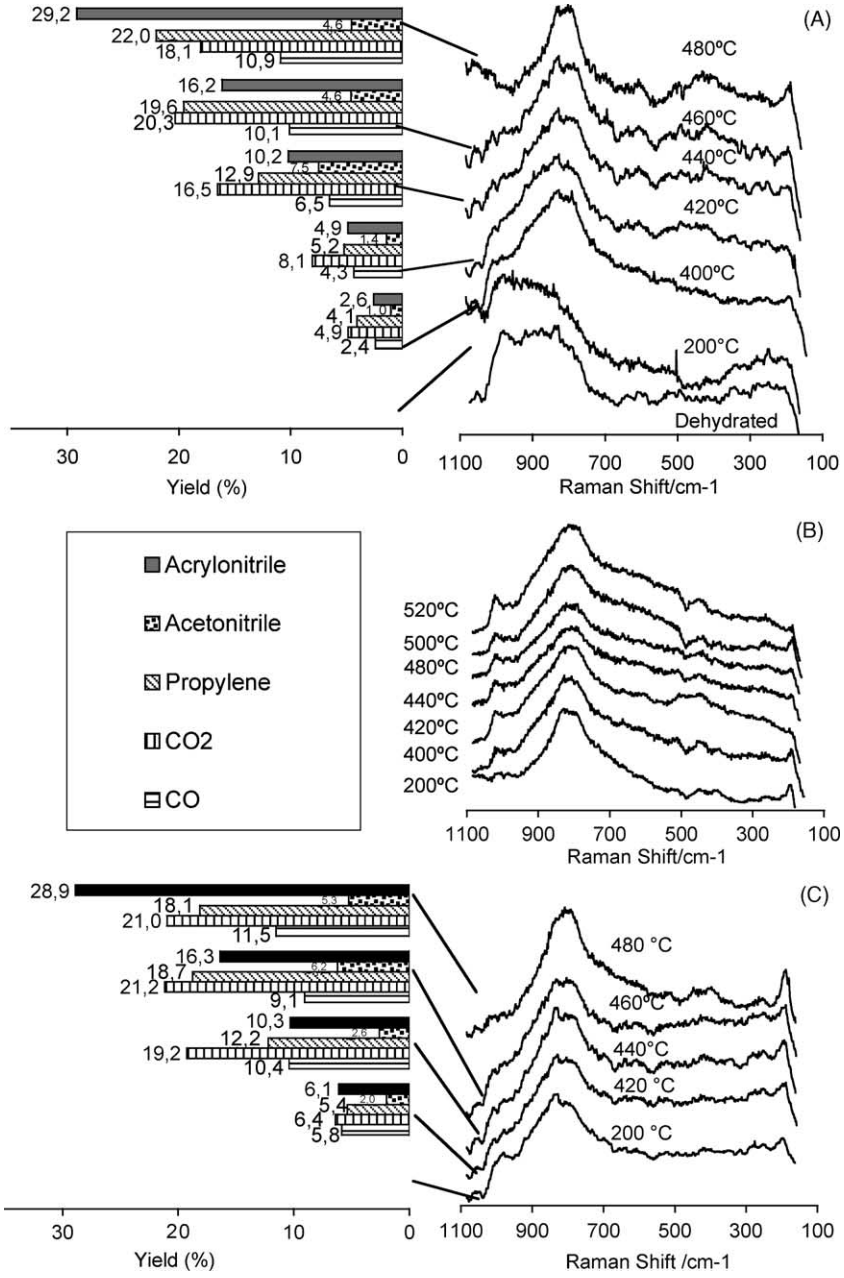

Fig. 3. *Operando* Raman spectra with product yields of 1Sb1V/Al-1 catalyst during propane ammoxidation (A, first run), under oxidizing conditions (B, O_2 + He) and during propane ammoxidation (C, second run). Reaction conditions: 200 mg of catalyst and total flow 20 ml/min.

The structural transformations observed during propane ammoxidation indicate that, during ammoxidation, surface vanadium (V) species reduce to V(III) into $VSbO_4$. The ammoxidation reaction feed is not reducing, but it does not have a net oxidizing character either; heating under such conditions affords some reduction by generation of oxygen defects. The reduction of mixed Sb-V-O phases in inert atmospheres upon heating has been described elsewhere [11,24–26]. To see how reversible such transformation is, we run an in situ reoxidation. Thus, after reaction in the *operando* Raman system, the $1Sb_1V/Al$-1 catalyst was cooled to 200 °C. The ammoxidation feed was replaced by an oxidizing feed (oxygen in helium) and the catalyst was heated under such oxidizing atmosphere (TPO-Raman). Fig. 3B shows representative spectra. The $VSbO_4$ phase is stable during reoxidation; however, segregated vanadium and antimony species undergo transformations. The appearance of the Raman band at 1020 cm^{-1} shows that surface vanadium oxide species are progressively restored. The weak Raman feature at 190 cm^{-1} (α-Sb_2O_4) decreases as surface vanadium (V) species are restored. Such trend for surface vanadium and α-Sb_2O_4 species is opposite to the one observed during ammoxidation reaction (Fig. 3A). Therefore, the changes that occur on the catalyst during propane ammoxidation appear partially reversible upon reoxidation, which restores dispersed V(V) species.

To obtain additional insight about the catalytic species involved in the reaction cycle, a second ammoxidation run was carried out in the *operando* Raman–GC system, Thus, propane ammoxidation is run again on the $1Sb_1V/Al$-1catalyst, Fig. 3C shows representative Raman spectra and *simultaneous* activity results, measured on-line. During this run, the molecular structures of surface species are different since $VSbO_4$ phase is present before the catalytic reaction becomes measurable. It is interesting to compare the performance during the first and second run at 420 °C since neither $VSbO_4$ nor α-Sb_2O_4 are present during the first run at 420 °C (Fig. 3A). Both systems are active for propane ammoxidation, but the conversion to acrylonitrile is higher during the second run (6.1% versus 4.9% yield). This would be indicative of the role of $VSbO_4$, which would account for the better propane ammoxidation performance. The acrylonitrile yields at 440 °C and above are equivalent to those recorded during the first run. This is consistent with the similar molecular structures present in both runs under such conditions. However, it is interesting to underline that the production of propylene is lower during he second run. Propylene yield decreases by 18% at 480 °C, while CO_2 yield increases nearly by 17% at 480 °C.

4. Discussion

The ammoxidation reaction feed ($NH_3 + C_3H_8 + O_2 + He$) composition does not have a net reducing or oxidizing character. Such feed may promote partial reduction of the system by defect generation as temperature increases. These phenomena promote the interaction between Sb and V species [11,24–26]. Surface vanadium (V) reduces to V(III) under such conditions and stabilizes into $VSbO_4$. This is consistent with the oxidation states in $VSbO_4$, where Sb(V) and V(III) have been identified by Mössbauer and EPR spectroscopy, respectively [35,36]. The presence of Sb in $VSbO_4$ as Sb(V) only has also been determined by XPS [33]. α-Sb_2O_4 is a mixed-valence oxide that possesses Sb(III) and Sb(V) sites [35,36]. The conversion of surface V(V) oxide species into V(III) species in $VSbO_4$ during propane ammoxidation and the restoration of V(V) species upon reoxidation is in agreement with the enhancement of the redox properties of vanadium oxide when combined with antimony oxide [37–39] and with the dynamic character of $VSbO_4$ phases [26,27] and may facilitate a redox cycle for vanadium.

4.1. Catalytic cycle

V(V) species integrate in $VSbO_4$ as V(III) and Sb species segregate as α-Sb_2O_4 during ammoxidation and vice versa during reoxidation. This trend is consistently observed for the alumina-supported Sb-V oxide catalyst with different total Sb + V coverage on alumina and at different Sb/V atomic ratios [15,32]. $VSbO_4$ appears to facilitate those transformations since it accepts many stoichiometries around $V_1Sb_1O_4$

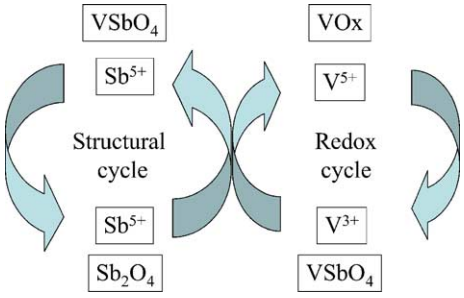

Scheme 3. Possible catalytic redox cycle of vanadium and migration cycle of antimony during propane ammoxidation in V-Sb-O catalysts.

[26,27]. Thus, V sites may undergo a redox cycle involving surface vanadium (V) species and bulk vanadium (III) species, which is facilitated by the reversible migration of Sb(V) species to and from segregated Sb oxide phase (Scheme 3). Accordingly, the incorporation of V(III) into $VSbO_4$ results in higher amount of segregated α-Sb_2O_4. The presence of surface V(V) species on the surface, will create a deficit of cations (V(III)) that is compensated by the incorporation of Sb(V) cations. Such promotion of the redox properties of V species by segregated Sb results from the interaction between $VSbO_4$ and Sb_2O_4. The *operando* Raman–GC study provides an evidence of the proposed role of supra-surface antimony migrating between α-Sb_2O_4 and $VSbO_4$ in working catalysts [13]. *Such cooperation must endow the vanadium sites with rather unique redox properties*.

4.2. Surface vanadium sites

$VSbO_4$ is necessary for propane ammoxidation. The presence of surface vanadium oxide species during ammoxidation reaction accounts for higher propane activation [9,13,40]. An *operando* Raman–GC study in alumina-supported Sb-V-O catalyst suggests that the surface vanadium oxide species account for better conversion of propane to acrylonitrile, despite a lower selectivity due to propylene formation [2]. Propylene is a reaction intermediate in propane ammoxidation and its formation is related to surface vanadium oxide species [9,40,41]; thus, a large excess of surface vanadium oxide species may shift the reaction towards propylene formation [2]. For a given Sb/V atomic ratio, the use of a tartrate soluble Sb precursor (method **2**) affords a more efficient Sb-V interaction than the use of an Sb oxide suspension (method **1**). It is interesting to compare catalyst $1Sb_1V/Al$-1 at 420 °C during the first and second ammoxidation run (Fig. 3A and C). The conversion to acrylonitrile is higher in the second run, where $VSbO_4$ phase is present. The poor formation of $VSbO_4$ phase in the first run at 420 °C must account for its lower performance for propane ammoxidation. At 480 °C both runs afford nearly the same conversion to acrylonitrile (ca. 29% yield). The lower conversion to propylene during the second run (18% versus 22% yield) could be due to a more extensive Sb-V interaction that would result in a lower proportion of surface

vanadium oxide species. This is consistent with the oxidative dehydrogenation activity of Sb-V-O catalysts with excess of vanadium [40]. Such trend underlines the relevance of Sb-V interaction, which is maximum when a soluble Sb precursor is used. Therefore, the catalyst $1Sb_1V/Al$-2 affords a better conversion of propane to acrylonitrile (31.3% versus 28.1% yield) with a significantly better selectivity (51.1% versus 33.3%), mainly due to the lower conversion to propylene (11.6% versus 20.6 % yield), when compared to $1Sb_1V/Al$-1. Thus, the total conversion is lower in $1Sb_1V/Al$-2 (61.3%) versus $1Sb_1V/Al$-1 (84.4%); but it is due to a lower formation of undesired acetonitrile, propylene, CO and CO_2, which makes $1Sb_1V/Al$-2 highly selective. A large excess of Sb would afford a selective system, but total activity would be low. Excess of surface vanadium oxides species would afford higher conversion of propane, but conversion to propylene and CO_x would compete with the conversion to acrylonitrile. An appropriate amount of surface vanadium oxide species on $VSbO_4$ affords the most efficient conversion of propane to acrylonitrile. At Sb/V = 1/1 atomic ratio, method **1** forms $VSbO_4$ during ammoxidation, but the feeble Sb-V interaction affords and excessive population of surface vanadium oxides species; on the other hand, method **2** maximizes the Sb-V interaction, thus allowing a number of surface vanadium oxide species that must be in equilibrium with bulk vanadium species in $VSbO_4$. These sites are highly efficient for propane ammoxidation.

5. Conclusions

The use of a soluble Sb precursor instead of a Sb_2O_3 suspension maximizes the Sb-V interaction and the $VSbO_4$ phase is formed during calcination. In the former, the amount of surface vanadium oxide species must be in equilibrium with bulk vanadium in $VSbO_4$, which makes the catalyst more selective and efficient for acrylonitrile production. The *operando* Raman–GC study shows cooperation between surface vanadia, segregated antimony oxide and $VSbO_4$. Surface V(V) oxide species in equilibrium with V(III) species in bulk $VSbO_4$ account for the redox cycle, which is facilitated by a migration cycle of Sb(V) species from segregated antimony oxide phase to $VSbO_4$.

Acknowledgments

This research was funded by MCyT (Spain) project MAT-2002-0400-C02-01 and CICYT (Spain) project QUI98-0784, co-funded by Repsol-YPF (Spain). CICYT (Spain) Grant IN96-0053 partially funded the acquisition of the Raman system. M.O.G.-P. thanks the Ministry of Science and Technology of Spain, for a doctorate studies fellowship. The authors thank the support of Mr. Ramón Tomé Neches and Mr. Francisco Izquierdo Galve for their help and suggestions during the fabrication of the *operando* cell at the Institute of Catalysis and Petroleumchemistry, CSIC, in Madrid.

References

[1] B.M. Weckhuysen, Chem. Commun. (2002) 97, Reference 11.
[2] M.A. Bañares, M.O. Guerrero-Pérez, J.L.G. Fierro, G.G. Cortez, J. Mater. Chem. 12 (2002) 3337.
[3] M.O. Guerrero-Pérez, M.A. Bañares, Chem. Commun. (2002) 1292.
[4] M.A. Bañares, I.E. Wachs, J. Raman Spectrosc. 33 (2002) 359.
[5] G. García-Cortez, M.A. Bañares, J. Catal. 209 (2002) 435.
[6] G. Mul, M.A. Bañares, G. Garcia Cortez, B. van der Linden, S.J. Khatib, J.A. Moulijn, Phys. Chem. Chem. Phys. 5 (2003) 4378.
[7] J.F. Brazdil, J.P. Bartek, US Patent 5,854,172 (1998);
J.F. Brazdil, F.A.P. Kobarvkantei, J.P. Padolwski, JP Patent 11033399 (1999);
A.T. Guttmann, R.K. Grasselli, F.J. Brazdil, US Patents 4,746,641; 4,788,173; 4,837,233 (1988).
[8] D.D. Sureh, D.A. Ornoff, J.F. Brazdil, L.C. Glaeser, M.S. Friendich, US Patent 4,7060,159 (1988);
L.C. Glaeser, J.F. Brazdil, M.A. Toft, US Patents 4,843,655; 4,835,125 y 4,837,192 (1988).
[9] A. Andersson, S.L.T. Andersson, G. Centi, R.K. Grasselli, M. Sanati, F. Trifirò, Stud. Surf. Sci. Catal. 75 (1993) 691.
[10] R.K. Grasselli, Catal. Today 49 (1999) 141.
[11] G. Centi, S. Perathoner, F. Trifirò, Appl. Catal. A 157 (1997) 143.
[12] R.K. Grasselli, Top. Catal. 15 (2001) 93.
[13] R.K. Grasselli, in: G. Ertl, H. Knözinger, J. Weitkamp (Eds.), Handbook of Heterogeneous Catalysis, vol. V, 1997, p. 2303.
[14] O. Ratajczak, H.W. Zanthoff, S. Geisler, Stud. Surf. Sci. Catal. 130 (2000) 1685.
[15] M.O. Guerrero-Pérez, J.L.G. Fierro, M.A. Vicente, M.A. Bañares, J. Catal. 206 (2002) 339.
[16] L.C. Brazdil, A.M. Ebner, J.F. Brazdil, J. Catal. 163 (1996) 117.
[17] J. Nilsson, A.R. Landa Cánovas, S. Hansen, A.J. Andersson, J. Catal. 160 (1996) 244.
[18] J. Nilsson, A.R. Landa Cánovas, S. Hansen, A.J. Andersson, J. Catal. 186 (1999) 442.
[19] G. Centi, P. Mazzoli, S. Perathoner, Appl. Catal. A 165 (1997) 273.
[20] S. Anderson, A. Hansen, Wickman, Top. Catal. 15 (2001) 103.
[21] J. Nilsson, A.R. Landa Cánovas, S. Hansen, A.J. Andersson, Catal. Today 33 (1997) 97.
[22] R. Nilsson, T. Lindblad, A. Andersson, C. Song, S. Hansen. New Developments in Selective Oxidation II (1994) 293.
[23] G. Centi, P. Mazzoli, Catal. Today 28 (1996) 351.
[24] G. Centi, S. Perathoner, App. Catal. A Gen. 124 (1995) 317.
[25] R.G. Teller, M.R. Antonio, J.F. Brazdil, R.K. Grasselli, J. Solid State Chem. 64 (1986) 249.
[26] J.F. Brazdil, M.A. Toft, J.P. Bartek, R.G. Teller, R.M. Cyngier, Chem. Mater. 10 (1998) 4100.
[27] H.W. Zanthoff, W. Grünert, S. Bucholz, M. Heber, L. Stievano, F.E. Wagner, G.U. Wolft, J. Mol. Catal. A 162 (2000) 443.
[28] M.O. Guerrero-Pérez, J.L.G. Fierro, M.A. Bañares, unpublished results.
[29] I.E. Wachs, L.E. Briand, J.M. Jehng, L. Burcham, X. Gao, Catal. Today 57 (2000) 323.
[30] I.R. Lewis (Ed.), Handbook of Raman Spectroscopy. From the Research Laboratory to the Process Line, Marcel Dekker Inc., New York, 2001.
[31] J.R. Ferraro, K. Nakamoto, Introductory Raman Spectroscopy, Academic Press, New York, 1994.
[32] M.O. Guerrero-Perez, Ph.D. Dissertation, Universidad Autónoma de Madrid, Spain, 2003.

[33] M.O. Guerrero-Pérez, M.A. Vicente, J.L.G. Fierro, M.A. Bañares, submitted for publication.
[34] L. Burcham, G. Deo, X. Gao, I.E. Wachs, Top. Catal. 11–12 (2000) 85.
[35] T. Birchall, A.W. Sleight, Inorg. Chem. 15 (1976) 868.
[36] F.J. Berry, M.E. Brett, Inorg. Chim. Acta 7 (1983) L205.
[37] V.Y. Bychkov, M.Y. Sinev, V.P. Vislovskii, Kinet. Catal. 42 (2001) 574.
[38] V.P. Vislovskii, N.T. Shamilov, A.M. Sardarly, V.Yu. Bychkov, M.Yu. Sinev, P. Ruiz, R.X. Valenzuela, V. Cortés-Corberán, Chem. Eng. J. 95 (2003) 37.
[39] F. Barbieri, D. Cauzzi, F. De Smet, M. Devillers, P. Moggi, G. Predieri, P. Ruíz, Catal. Today 61 (2000) 353.
[40] R. Nilsson, T. Lindblad, A. Andersson, J. Catal. 148 (1994) 501.
[41] R. Catani, G. Centi, F. Trifirò, R.K. Grasselli, Ind. Eng. Chem. Res 31 (1992) 10.